

issn 0065-3713

INSTITUT D'AERONOMIE SPATIALE DE BELGIQUE

3 - Avenue Circulaire  
B - 1180 BRUXELLES

# AERONOMICA ACTA

A - N° 308 - 1986

The effect of saturn's rings on the upper-boundary insolation  
of its atmosphere

by

E. VAN HEMELRIJCK

BELGISCH INSTITUUT VOOR RUIMTE-AERONOMIE

3 - Ringlaan  
B - 1180 BRUSSEL

## FOREWORD

The paper "The effect of Saturn's rings on the upper-boundary insolation of its atmosphere" will be published in "Earth, Moon, and Planets", 1986.

## AVANT-PROPOS

L'article "The effect of Saturn's rings on the upper-boundary insolation of its atmosphere" sera publié dans "Earth, Moon, and Planets", 1986.

## VOORWOORD

De tekst "The effect of Saturn's rings on the upper-boundary insolation of its atmosphere" zal verschijnen in "Earth, Moon, and Planets", 1986.

## VORWORT

Der Text "The effect of Saturn's rings on the upper-boundary insolation of its atmosphere" wird in "Earth, Moon, and Planets", 1986 herausgegeben werden.

THE EFFECT OF SATURN'S RINGS ON THE UPPER-BOUNDARY INSOLATION  
OF ITS ATMOSPHERE

by

E. VAN HEMELRIJCK

Abstract

In this paper, the daily solar radiation incident at the top of Saturn's atmosphere and taking into account both the oblateness of the planet and the shadow of the ring system is calculated. It is found that the decrease of the daily insolation in winter is important near the solstices up to mid-latitudes and in the neighborhood of the equinoxes for equatorial and low latitudes. The combined effect of Saturn's rings and its flattening on the mean winter and annual daily insolation is also studied. The numerical results show that the mean wintertime insolation falls gradually in the (0-20°) latitude region to a peak value of about 50%. Beyond 20° the loss of insolation decreases and from approximately 45° up to polar region latitudes the decrease reaches a practically constant level of 35%. The mean annual daily insolation is maximally reduced by about 20% at localities of 20°.

## Résumé

Dans ce travail l'insolation diurne au sommet de l'atmosphère de Saturne est calculée. Aussi bien l'influence de l'aplatissement que l'effet d'ombre du système des anneaux ont été considérés. La diminution de l'insolation diurne en hiver est importante 1) à proximité du solstice jusqu'à des latitudes moyennes et 2) à proximité de l'équinoxe à des latitudes équatoriales et à basses latitudes. L'effet combiné des anneaux de Saturne et son aplatissement sur l'insolation diurne moyenne annuelle et en hiver a également été étudié. Les résultats numériques indiquent qu'en hiver l'insolation diurne moyenne diminue progressivement dans le domaine de latitude ( $0-20^\circ$ ) jusqu'à une valeur maximale d'environ 50%. Au-dessus de  $20^\circ$  la perte d'énergie solaire diminue et à partir de  $45^\circ$  jusque dans la région polaire la perte reste pratiquement constante d'environ 35%. La diminution de l'insolation diurne moyenne annuelle atteint une valeur d'environ 20% à une latitude de  $20^\circ$ .

## Samenvatting

In dit werk wordt de dagelijkse zonnestraling invallend aan de top van de atmosfeer van Saturnus berekend. Zowel de invloed van de afplatting als het schaduweffect van het ringensysteem werd in aanmerking genomen. De vermindering van de dagelijkse zonnestraling in de winter is belangrijk 1) in de omgeving van het solstitium tot op gemiddelde breedten en 2) in de nabijheid van het equinoctium op evenaarsbreedten en op lage breedten. Het gecombineerde effect van de ringen van Saturnus en zijn afplatting op de gemiddelde winterse en jaarlijkse dagelijkse zonnestralingen werd eveneens bestudeerd. De numerieke resultaten tonen aan dat in de winter de gemiddelde dagelijkse zonnestraling geleidelijk vermindert in het (0-20°) breedte-gebied tot een maximale waarde van ongeveer 50%. Boven de 20° vermindert het verlies aan zonne-energie en vanaf ongeveer 45° tot in het poolgebied blijft het verlies praktisch konstant op ongeveer 35%. De vermindering van de gemiddelde jaarlijkse dagelijkse zonnestraling bereikt een waarde van om en bij de 20% op een breedte van 20°.

## Zusammenfassung

In dieser Arbeit wird die tägliche Sonnenstrahlung am Rand der Atmosphäre des Saturnes berechnet. Der Einfluss der Abplattung wie auch der Schatteneffekt des Ringensystemes wurden berücksichtigt. Die Verminderung der täglichen Sonnenstrahlung in Winter ist wichtig 1) in der Umgebung des Solstitiums auf mittleren Breiten und 2) in der Umgebung des Äquinoktiums auf Äquatorbreiten und auf geringen Breiten. Das kombinierte Effekt der Ringen des Saturnes und seine Abplattung auf der mittleren jährlichen und winterlichen täglichen Sonnenstrahlung wurde auch studiert. Die numerische Resultaten zeigen dass in Winter die mittlere tägliche Sonnenstrahlung allmählich vermindert im (0-20°) Breitegebiet bis ein Höchstwert von ungefähr 50%. Über die 20° vermindert der Verlust in Sonnenenergie und von ungefähr 45° ab bis im Polgebiet bleibt der Verlust praktisch konstant mit einem Wert von ungefähr 35%. Die Verminderung der mittleren jährlichen täglichen Sonnenstrahlung erreicht ein Wert von ungefähr 20% auf einer Breite von 20°.

## 1. INTRODUCTION

The effect of the major rings (A, B and C) on the direct solar radiation at the top of Saturn's atmosphere has been calculated and briefly discussed by Brinkman and Mc Gregor (1979). The oblateness of the planet was also taken into account.

In their paper, the data for the Saturnian ring system (inner radius, outer radius and optical depth) were taken from Allen (1963) and Cook and Franklin (1973). Since the encounter of the Voyager spacecrafts with the planet, new and more accurate data for the distances from Saturn and the optical thickness are available. Although most of the values used by Brinkman and Mc Gregor (1979) are close to the more recent ones, it is to be emphasized that the B-ring optical depth is found to be higher than previously published values, the difference being of the order of 20 (inner B-ring) to approximately 80% (outer B-ring) (Esposito et al., 1983). The exact value of the effective B-ring optical thickness is, however, poorly determined due to the presence of relatively small regions of extremely low optical depths within an overall highly opaque layer (Smith et al., 1981).

The present work differs from that of Brinkman and Mc Gregor (1979) in that the rings are divided into two (A and C) or three (B) regions of different optical thicknesses and that we also took into consideration the Cassini division which has been ignored by the above mentioned authors. (The other rings are neglected because they are assumed to be transparent). Moreover, our calculations are based on the data recently published by Esposito et al. (1983). It has also to be noticed that in the paper of Brinkman and Mc Gregor (1979) some expressions were slightly in error.

In a first section we briefly present the calculation scheme for the upper-boundary insolation including the flattening effect and the shadow effect of the ring system. Then, taking into account the planetary and orbital data of Saturn, we determine the daily insolation and the mean (summer, winter or annual) daily insolations. In the Figures, the incident solar radiations are given in calories per square centimeter per Saturnian day; insolation values expressed in Watt per square meter may be obtained by multiplying the unit used by a factor of about 0.484.

## 2. CALCULATION SCHEME FOR THE DAILY INSOLATION

In calculating the ring contribution, the rings are treated as infinitely thin, homogeneous annuli and are assumed to be in the equatorial plane.

We have followed the method of Brinkman and Mc Gregor (1979) in adopting a rectangular coordinate system : the z-axis coincide with the spin axis of the planet, the y-axis is perpendicular to the Sun's rays and the x-axis is defined so as to form a right handed coordinate system. The origin 0 is located in the center of the planet and  $z = 0$  represents the expression of the equator.

The coordinates of a point P on the rings may now be written under the following forms :

$$x = R \cos \alpha \quad (1)$$

$$y = R \sin \alpha \quad (2)$$

$$z = 0 \quad (3)$$



where  $R$  is the radial distance (in units of Saturn radii  $R_S \approx 60000$  km) of  $P$  from the origin  $O$  and  $\alpha$  is the angle between the line connecting the point to the origin and the  $x$ -axis.

For an oblate planet, characterized by a flattening  $f$ , the line throughout  $P$  and parallel to the Sun's rays intersects the planet at the point  $S$ , the coordinates of which are given by :

$$x_S = z_S \cot \delta_{\odot} + R \cos \alpha \quad (4)$$

$$y_S = R \sin \alpha \quad (5)$$

$$z_S =$$

$$\left\{ -R \cos \alpha \cot \delta_{\odot} \pm \left[ (R \cos \alpha \cot \delta_{\odot})^2 - [\cot^2 \delta_{\odot} + (1-f)^{-2}] (R^2 - 1) \right]^{1/2} \right\} / [\cot^2 \delta_{\odot} + (1-f)^{-2}] \quad (6)$$

where  $\delta_{\odot}$  is the solar declination.

Expression (6) can also be written as :

$$z_S =$$

$$\left\{ -R \cos \alpha \cot \delta_{\odot} \pm \left[ (R \cos \alpha \cot \delta_{\odot})^2 - (1.256 + \cot^2 \delta_{\odot}) (R^2 - 1) \right]^{1/2} \right\} / (1.256 + \cot^2 \delta_{\odot}) \quad (7)$$

where the factor 1.256 represents, in a very good approximation, the numerical value of the expression  $(1-f)^{-2}$  (see Table I).

In (6) or (7) the smallest absolute value has to be taken as z-coordinate, the largest one representing the theoretical intersection on the unilluminated side of the planet.

Furthermore, it is easy to see that the planetocentric latitude  $\varphi'$  and the longitude  $\lambda$  (with respect to the rotating x-axis) of the intersection point can be calculated using the following relations :

$$\varphi' = \text{atan} [z_S / (x_S^2 + y_S^2)^{1/2}] \quad (8)$$

$$\lambda = \text{atan} (y_S / x_S) \quad (9)$$

The shadow profiles, for a solar declination  $\delta_{\odot}$  (taken to be constant over a Saturnian day) and a radial distance R, can be determined by combining (4), (5), (7), (8) and (9).

The Sun's rays throughout points on the ring system for which

$$\alpha > \text{acos} \{ (\tan \delta_{\odot} / R) [(1.256 + \cot^2 \delta_{\odot})(R^2 - 1)]^{1/2} \} \quad (10)$$

do not intersect the planet. After rearrangement, equation (10) can also be written in a more simplified form as :

$$\alpha > \text{acos} [(1 + 1.256 \tan^2 \delta_{\odot})(1 - 1/R^2)]^{1/2} \quad (11)$$

The expression of a plane parallel to the equator, in terms of the planetocentric latitude  $\varphi'$  can be written as :

$$z = \pm (1.256 + \cot^2 \varphi')^{-1/2} \quad (12)$$

where the plus sign is used for the northern hemisphere ( $\varphi' > 0$ ), and the minus sign is taken for the southern one ( $\varphi' < 0$ ). The above mentioned plane intersects the shadow profiles for angles  $\alpha$  which are given by :

$$\alpha = \pm \arccos \left\{ \frac{[(1.256 + \cot^2 \delta_{\odot}) (1.256 + \cot^2 \varphi')^{-1} + (R^2 - 1)]}{2R \cot \delta_{\odot} (1.256 + \cot^2 \varphi')^{1/2}} \right\} \quad (13)$$

Finally, relationships (4), (5), (7), (9) and (13) allow the integration angles for the calculation of the daily insolation to be determined for any declination angle  $\delta_{\odot}$  (or for any specific day) as a function of the planetocentric latitude  $\varphi'$  and the radial distance  $R$ .

The instantaneous insolation ( $I$ ) of the outer planets, neglecting the oblateness effect or any other effect, may be expressed as (see e.g. Ward, 1974; Vorob'yev and Monin, 1975; Levine et al., 1977; Van Hemelrijck, 1982a, b, c, 1983a) :

$$I = S \cos z' \quad (14)$$

with

$$S = S_{\odot} / r_{\odot}^2 \quad (15)$$

and

$$r_{\odot} = a_{\odot} (1 - e^2) / (1 + e \cos W) \quad (16)$$

In expressions (14) to (16)  $S$ ,  $z'$ ,  $S_{\odot}$ ,  $a_{\odot}$ ,  $e$  and  $W$  are respectively the solar flux at an heliocentric distance  $r_{\odot}$ , the zenith angle of the incident solar radiation, the solar constant at the mean Sun-Earth distance of 1 AU taken at  $1.96 \text{ cal cm}^{-2} (\text{min})^{-1}$  (Wilson, 1982), the planet's semimajor axis, the eccentricity and the true anomaly which is given by :

$$W = \lambda_{\odot} - \lambda_P \quad (17)$$

where  $\lambda_{\odot}$  and  $\lambda_P$  are the planetocentric longitude of the Sun (called solar longitude in the figures) and the planetocentric longitude of the planet's perihelion.

For a spherical planet, the cosine of the zenith angle  $z'$  may be written as :

$$\cos z' = \sin \varphi' \sin \delta_{\odot} + \cos \varphi' \cos \delta_{\odot} \cos h \quad (18)$$

where  $h$  is the local hour angle of the Sun;  $\delta_{\odot}$  can be computed from the relation :

$$\sin \delta_{\odot} = \sin \epsilon \sin \lambda_{\odot} \quad (19)$$

The daily insolation  $I_D$  (see also Van Hemelrijck 1983b, 1985b) can now be obtained by integrating relation (14) over time during the light time of the day and is given by :

$$I_D = (ST/\pi) (h_0 \sin \varphi' \sin \delta_{\odot} + \sin h_0 \cos \varphi' \cos \delta_{\odot}) \quad (20)$$

where  $T$  is the sidereal day and where the local hour angle at sunrise (or sunset)  $h_{\odot}$  may be determined from :

$$h_{\odot} = \text{acos} (- \tan \delta_{\odot} \tan \varphi') \quad (21)$$

if

$$|\varphi'| < \pi/2 - |\delta_{\odot}|$$

In regions where there is no sunrise ( $\varphi' < -\pi/2 + \delta_{\odot}$  or  $\varphi' > \pi/2 + \delta_{\odot}$ ) we have  $h_{\odot} = 0$ ; in regions where the Sun remains above the horizon all day ( $\varphi' > \pi/2 - \delta_{\odot}$  or  $\varphi' < -\pi/2 - \delta_{\odot}$ ), we may put  $h_{\odot} = \pi$ .

Finally, the mean (summer, winter or annual) daily insulations, hereafter denoted as  $(\bar{I}_D)_S$ ,  $(\bar{I}_D)_W$  and  $(\bar{I}_D)_A$  respectively, may be found by integrating relation (14) within the appropriate time limits, yielding the total insolation over a season or a year, and by dividing the obtained result by the corresponding length of the summer ( $T_S$ ) or winter ( $T_W$ ) or tropical year ( $T_O$ ). For the calculation of  $T_S$  or  $T_W$  we refer to e.g. Van Hemelrijck (1982c).

In this paper, and for the northern hemisphere, the summer is arbitrary defined as running from vernal equinox over summer solstice to autumnal equinox and spanning  $180^\circ$ ; on the other hand, it is obvious that  $\lambda_{\odot} = 180^\circ$  and  $\lambda_{\odot} = 360^\circ$  mark the beginning and the end of the winter period. In the southern hemisphere, the solar longitude intervals  $(0 - 180^\circ)$  and  $(180 - 360^\circ)$  divide the year into astronomical winter and summer.

In the case of an oblate planet, there is an angle  $v = \varphi - \varphi'$ , the so-called angle of the vertical, between the planetographic latitude ( $\varphi$ ) and the planetocentric latitude ( $\varphi'$ ). In terms of the latter, this angle can be written as :

$$v = \text{atan}(1.256 \tan \varphi') - \varphi' \quad (22)$$

Defining  $Z$  as the zenith angle for an oblate planet, the following relation can be obtained by applying the formulas of spherical trigonometry (Van Hemelrijck, 1982a, b, 1983a) :

$$\cos Z = \cos v \cos z' + \sin v(-\tan \varphi' \cos z' + \sin \delta_{\odot} \sec \varphi') \quad (23)$$

The daily insolation of an oblate planet  $I_{DO}$  can now be obtained by integrating relation (14) within the appropriate time limits, where  $\cos z'$  has to be replaced by expression (23) yielding :

$$\begin{aligned} I_{DO} = (ST/\pi) \{ & \cos v(h_{\odot} \sin \varphi' \sin \delta_{\odot} + \sin h_{\odot} \cos \varphi' \cos \delta_{\odot}) \\ & + \sin v[-\tan \varphi' (h_{\odot} \sin \varphi' \sin \delta_{\odot} + \sin h_{\odot} \cos \varphi' \cos \delta_{\odot}) \\ & + h_{\odot} \sin \delta_{\odot} \sec \varphi'] \} \quad (24) \end{aligned}$$

where  $h_{\odot}$ , the local hour angle at rising or setting of the Sun for an oblate planet, is generally slightly different from  $h_{\odot}$ . As for a spherical planet,  $h_{\odot}$  may be derived from equation (23) which gives :

$$h_{\odot} = \text{acos}(-\tan \delta_{\odot} \tan \varphi) \quad (25)$$

which is similar to equation (21).

Obviously, in areas of permanent darkness and continuous sunlight we have  $h_{oo} = 0$  and  $h_{oo} = \pi$ , respectively.

The oblateness effect on the solar radiation at the top of the atmosphere of Saturn (and other planets) has been analyzed in detail by Van Hemelrijck (1982a). It has been found that the flattening causes significant variations in both the planetary-wide distribution and the intensity of the daily insolation and, of course, in the latitudinal variation of the mean daily insolations.

The shadows cast by the ring system of Saturn causes the insolation to decrease by an amount depending upon the latitude, the oblateness and the solar declination via  $\cos Z$  and evidently, upon the optical thickness ( $\tau$ ) of one or more than one rings (if there is no intersection or if a point on the planet is outside of any ring shadow it is clear that the optical depth equals zero).

The daily insolation  $I_{DO\tau}$ , taking into account both the shadow effect and the influence of the oblateness, may then be expressed as (Levine et al., 1977; Brinkman and Mc Gregor, 1979; Van Hemelrijck, 1985a) :

$$I_{DO\tau} = (ST/\pi) \int_0^{h_{oo}} \cos Z \exp(-\tau \sec Z) dh \quad (26)$$

In winter and for a given latitude it is evident that, in general, the integration interval ( $0 - h_{oo}$ ) has to be divided into two or more

regions depending upon the number of rings that, during the day, casts a shadow on the latitude under consideration. Furthermore, it is also obvious that  $\tau$ , figuring in expression (26), represents the optical thickness corresponding to the ring which attenuates the solar radiation.

The mean daily insolations  $(\bar{I}_{DO\tau})_A$ ,  $(\bar{I}_{DO\tau})_S$  and  $(\bar{I}_{DO\tau})_W$  may, as earlier, be found by integrating numerically equation (26) over the appropriate time periods.

Table I represents the numerical values of the orbital and planetary data (Van Hemelrijck, 1982a; Davies et al., 1983) used for the computations, whereas parameters for the ring system are given in Table II (Esposito et al., 1983). It has to be pointed out that  $T_S$  and  $T_W$ , figuring in Table I, represents the lengths of the summer and winter corresponding to the northern hemisphere. For the southern one, the two values have to be interchanged.

### 3. DISCUSSION OF CALCULATION

#### 3.1. Daily insolation

For the daily insolation, as already mentioned, we have followed the method adopted by e.g. Levine et al. (1977) and Brinkman and Mc Gregor (1979) in presenting our results in the form of contour maps giving the incident solar radiations in  $\text{cal cm}^{-2} (\text{Saturnian day})^{-1}$  as a function of latitude and heliocentric longitude of the Sun taken to be equal to  $0^\circ$  at the northern hemisphere vernal equinox.



TABLE I : Elements of the planetary orbit of Saturn.

Semimajor axis	$a_{\odot}$ (AU)	9.539
Eccentricity	$e$	0.05561
Longitude of perihelion	$\lambda_P$ ( $^{\circ}$ )	279.07
Obliquity	$\epsilon$ ( $^{\circ}$ )	26.73
Oblateness	$f$	0.1076209
Sidereal day	$T$ (Earth days)	0.44
Tropical year	$T_O$ ( " )	10759.20
Length of the summer	$T_S$ ( " )	5755.56
Length of the winter	$T_W$ ( " )	5003.64

TABLE II : Parameters of the ring system.

Region	Boundaries ( $R_S$ )	Mean $\tau$
Inner C	1.24 - 1.39	0.08
Outer C	1.39 - 1.52	0.15
Inner B	1.52 - 1.66	1.21
Middle B	1.66 - 1.72	1.76
Outer B	1.72 - 1.95	1.84
Cassini	1.95 - 2.02	0.12
Inner A	2.02 - 2.16	0.70
Outer A	2.16 - 2.27	0.57

Figure 1 illustrates the latitudinal and seasonal distribution of the daily insolation (see also Vorob'yev and Monin, 1975 and Levine et al., 1979). The planet is considered as a sphere and the influence of the ring system is neglected. The calculations reveal that the maximum solar radiations occur near the solstices. This is due to the fact that the perihelion position  $\lambda_p$  is located in the vicinity of the south summer solstice. The insolation at the solstices reaches about 5.5 (north pole) and 6.8 (south pole) cal. cm<sup>-2</sup> (Saturnian day)<sup>-1</sup>. The ratio of both insolutions, in terms of  $e$  and  $\lambda_p$ , may be expressed as (Van Hemelrijck, 1982c) :

$$(I_D)_{NP(ss)} / (I_D)_{SP(ss)} = [(1 + e \sin \lambda_p) / (1 - e \sin \lambda_p)]^2 \quad (27)$$

where the subscripts NP, SP and ss refer respectively to the north pole, the south pole and the summer solstices. Expression (27) indicates that  $(I_D)_{NP(ss)} < (I_D)_{SP(ss)}$  if  $\pi < \lambda_p < 2\pi$  which is true not only for Saturn, but also for the Earth ( $\lambda_p = 282^\circ$ ) and Mars ( $248^\circ$ ). For the outer planets Jupiter, Uranus and Neptune the opposite effect is found.

The ratio of the polar solar radiation at summer solstice  $(I_D)_{P(ss)}$  to the equatorial one  $(I_D)_{E(ss)}$  can be written by the well-known relationship :

$$(I_D)_{P(ss)} / (I_D)_{E(ss)} = \pi \tan \epsilon \quad (28)$$

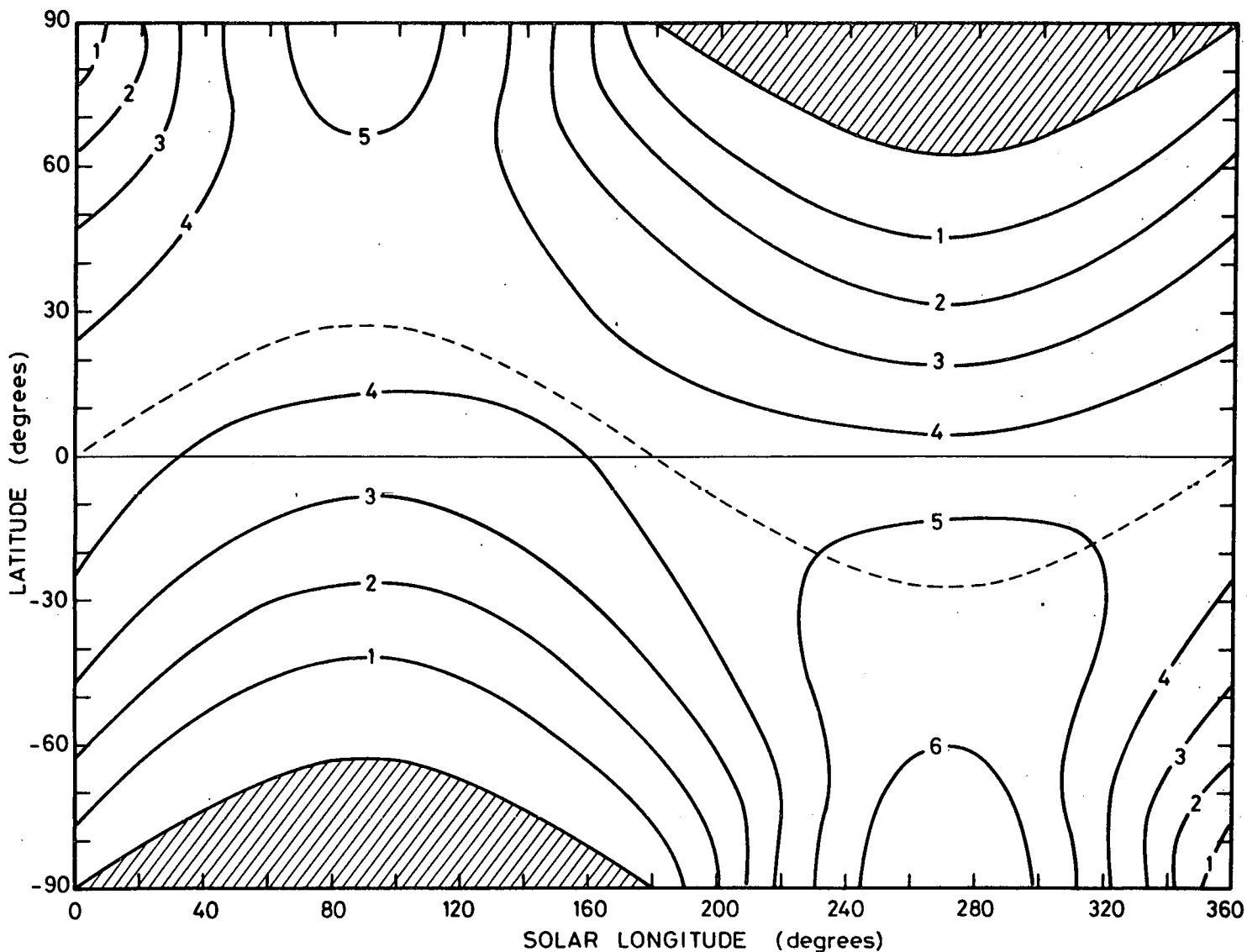


Fig. 1.- Seasonal and latitudinal variation of the daily insolation at the top of the atmosphere of Saturn. The planet is assumed to be spherical and the shadow effect of the ring system is neglected. Solar declination is represented by the dashed line. The areas of permanent darkness are shaded. Values of the daily insolation in calories per square centimeter per Saturnian day are given on each curve.

stating that  $(I_D)_{P(ss)} > (I_D)_{E(ss)}$  for  $\epsilon > 17.7$ . For Saturn, this ratio amounts to about 1.6. Based on the above mentioned values for the polar summer solstice insolation it follows that the corresponding equatorial insolation is approximately equal to  $3.5(\lambda_{\odot} = 90^\circ)$  and  $4.3(\lambda_{\odot} = 270^\circ)$  cal  $\text{cm}^{-2}$  (Saturnian day) $^{-1}$ .

One can also determine mathematically the solar longitude intervals where  $(I_D)_P > (I_D)_E$ . Indeed, from (20) it is easy to show that :

$$(I_D)_P / (I_D)_E = \pm \pi \tan \delta_{\odot} = \pm \pi \sin \epsilon \sin \lambda_{\odot} / (1 - \sin^2 \epsilon \sin^2 \lambda_{\odot})^{1/2} \quad (29)$$

the plus sign being used for the north pole, the minus sign for the southern one. Introducing  $\epsilon = 26.73$  in equation (29) it follows that, in the northern hemisphere,  $(I_D)_P > (I_D)_E$  if  $\lambda_{\odot}$  ranges from approximately  $42$  to  $138^\circ$ . In the southern hemisphere the polar daily insolation exceeds that of the equator in the approximate solar longitude interval ( $222 - 318^\circ$ ).

Finally in winter, as for practically all the outer planets, the isocontours closely parallel the curve limiting the area of no sunrise. In summer, the parallelism between the insolation contours and the line bounding the zone of continuous sunlight vanishes almost completely.

The seasonal and latitudinal variation of the solar radiation at the top of the Saturnian atmosphere, taking into account both the oblateness effect and the shadow effect of the ring system, is plotted in Figures 2 (northern winter hemisphere) and 3 (southern winter hemisphere). The insolation pattern for the summer period is not plotted because it can easily be seen that the summer hemispheres are not affected

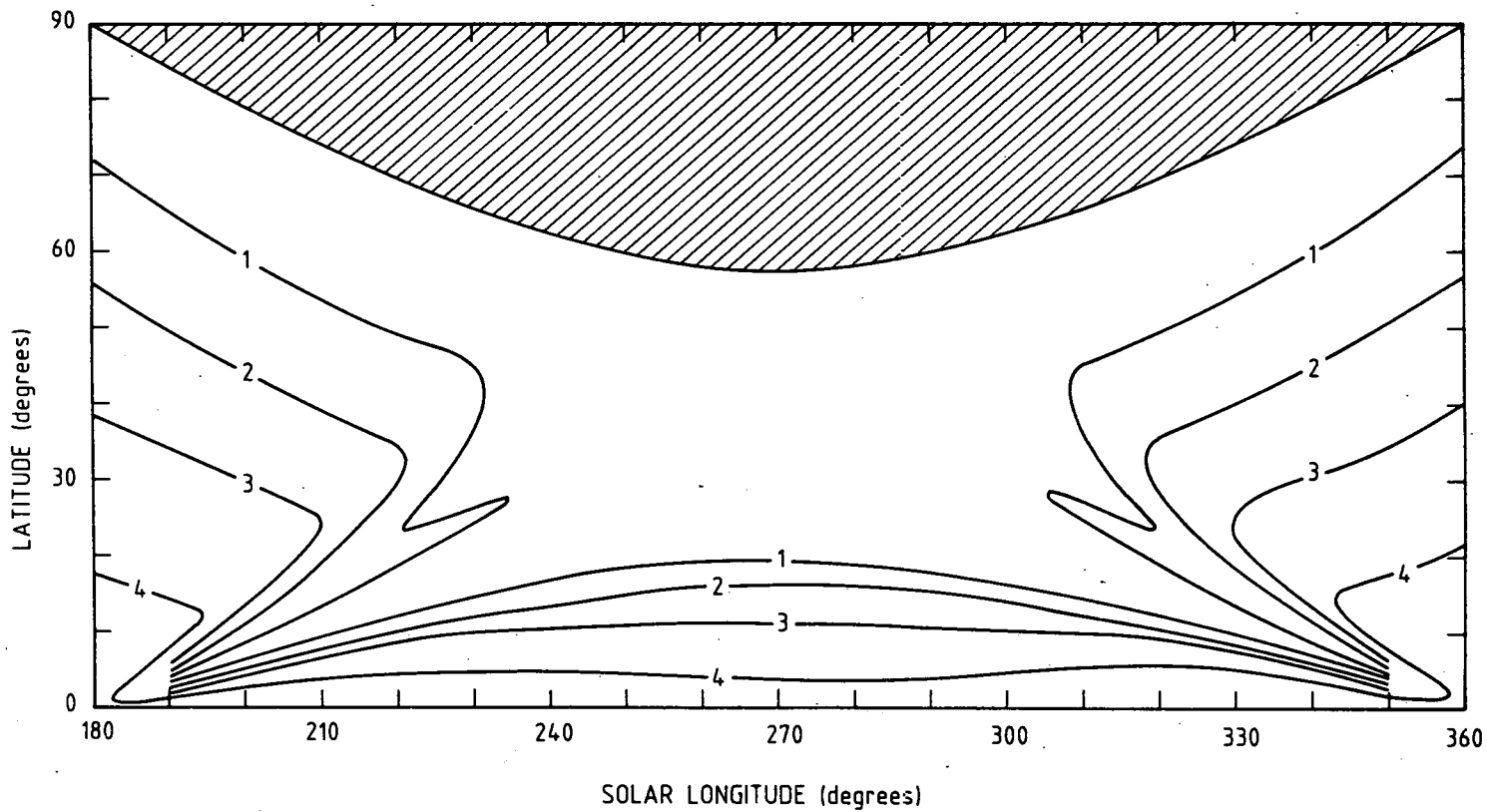


Fig. 2.- Seasonal and latitudinal variation of the daily insolation ( $I_{DO\tau}$ ) at the top of the atmosphere of Saturn (northern winter hemisphere). Both the oblateness effect and the shadow effect of the ring system are taken into account. See Fig. 1 for full explanation.

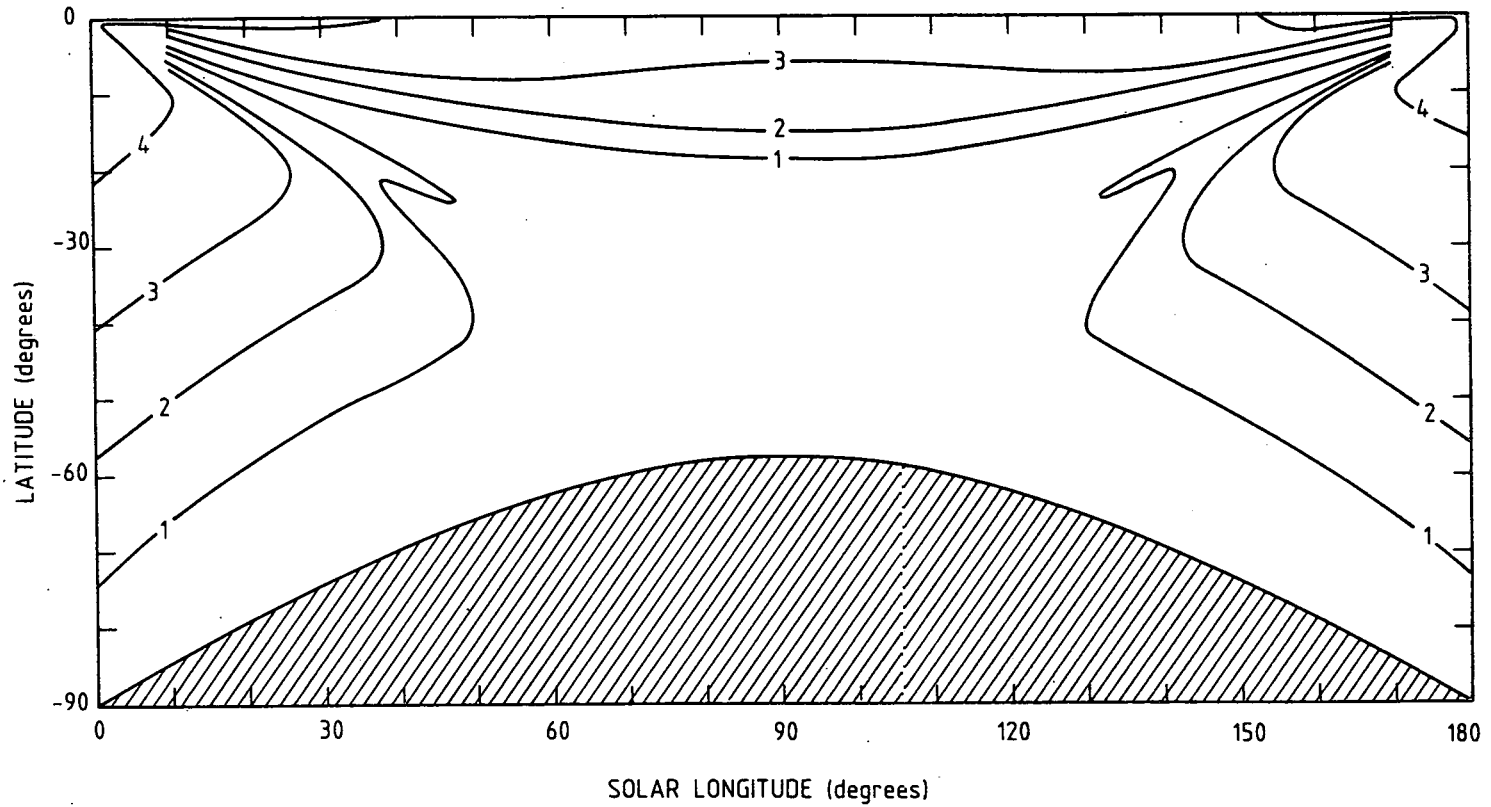


Fig. 3.- Seasonal and latitudinal variation of the daily insolation ( $I_{DO\tau}$ ) at the top of the atmosphere of Saturn (southern winter hemisphere). Both the oblateness effect and the shadow effect of the ring system are taken into account. See Fig. 1 for full explanation.

by the ring system. For the influence of the oblateness on the daily solar radiation in this region we refer to Van Hemelrijck (1982a). This paper reveals that the effect of the oblateness increases the insolation over much of the summer hemisphere, especially near summer solstice, where a rise of the incident solar radiation on the order of 3% has been found. In the neighborhood of the equinoxes there is a loss of insolation which is of most importance for the midlatitude regions.

Comparing Figure 1 with Figures 2 and 3, it is obvious that the ring system causes the daily solar radiation to decrease over an extensive part of the winter hemisphere. This characteristic feature is studied, in more details, in Figures 4, 5 and 6 presenting the latitudinal variation (for some specific values of the solar longitude) of the ratio of the daily insolation taking into account both the shadow effect and the oblateness effect ( $I_{DO\tau}$ ) to the daily insolation without those effects ( $I_D$ ) (full line). The ratio ( $I_{DO}/I_D$ ) (dashed line) is also given.

Near the autumnal equinoxes (Figure 4), where the solar declination ( $\delta_\odot$ ) is rather small, the shadows of the ring system are limited to equatorial latitudes and, as a consequence, the attenuation of the solar radiation is confined to this low latitudes. This phenomenon is clearly demonstrated in Figure 4 for a solar longitude of  $20^\circ$  (southern hemisphere) or  $200^\circ$  (northern hemisphere). The loss of insolation reaches a maximum at a latitude of approximately  $8^\circ$  and equals a factor of nearly 10. At a latitude of about  $20^\circ$  the curves representing the ratios ( $I_{DO\tau}/I_D$ ) and ( $I_{DO}/I_D$ ) coincide which means that the shadow effect is no more applicable to latitudes beyond the above mentioned one and for a solar position of  $20^\circ$  (or  $200^\circ$ ).



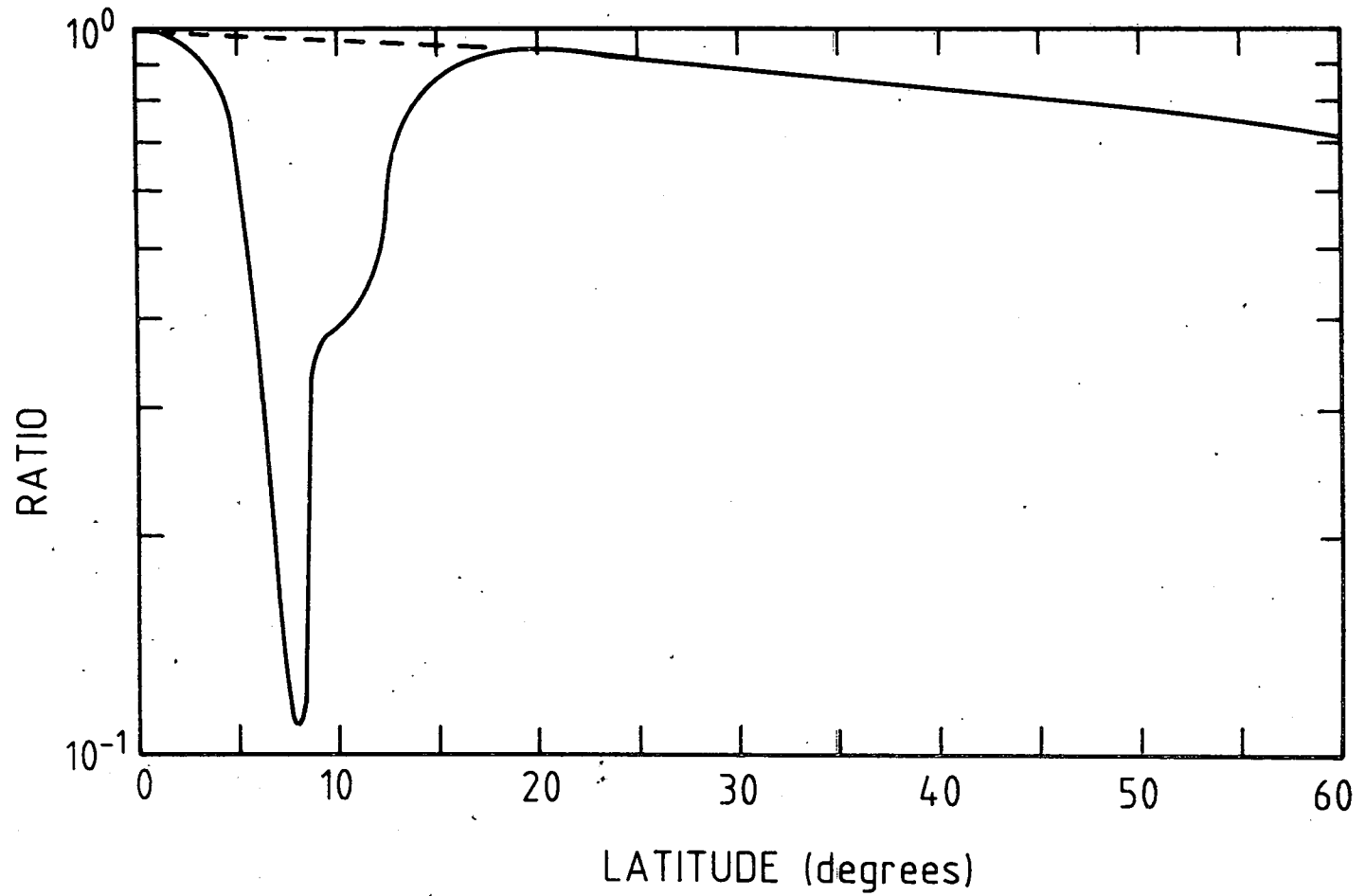


Fig. 4.- Latitudinal variation in the winter hemisphere at a solar longitude of  $20^\circ$  ( $200^\circ$ ) of the ratio of the daily insolation with the oblateness effect and the effect of the ring system ( $I_{DO\tau}$ ) to the daily insolation without the above mentioned effects ( $I_D$ ) (full line). The ratio ( $I_{DO}/I_D$ ) is also represented (dashed curve).

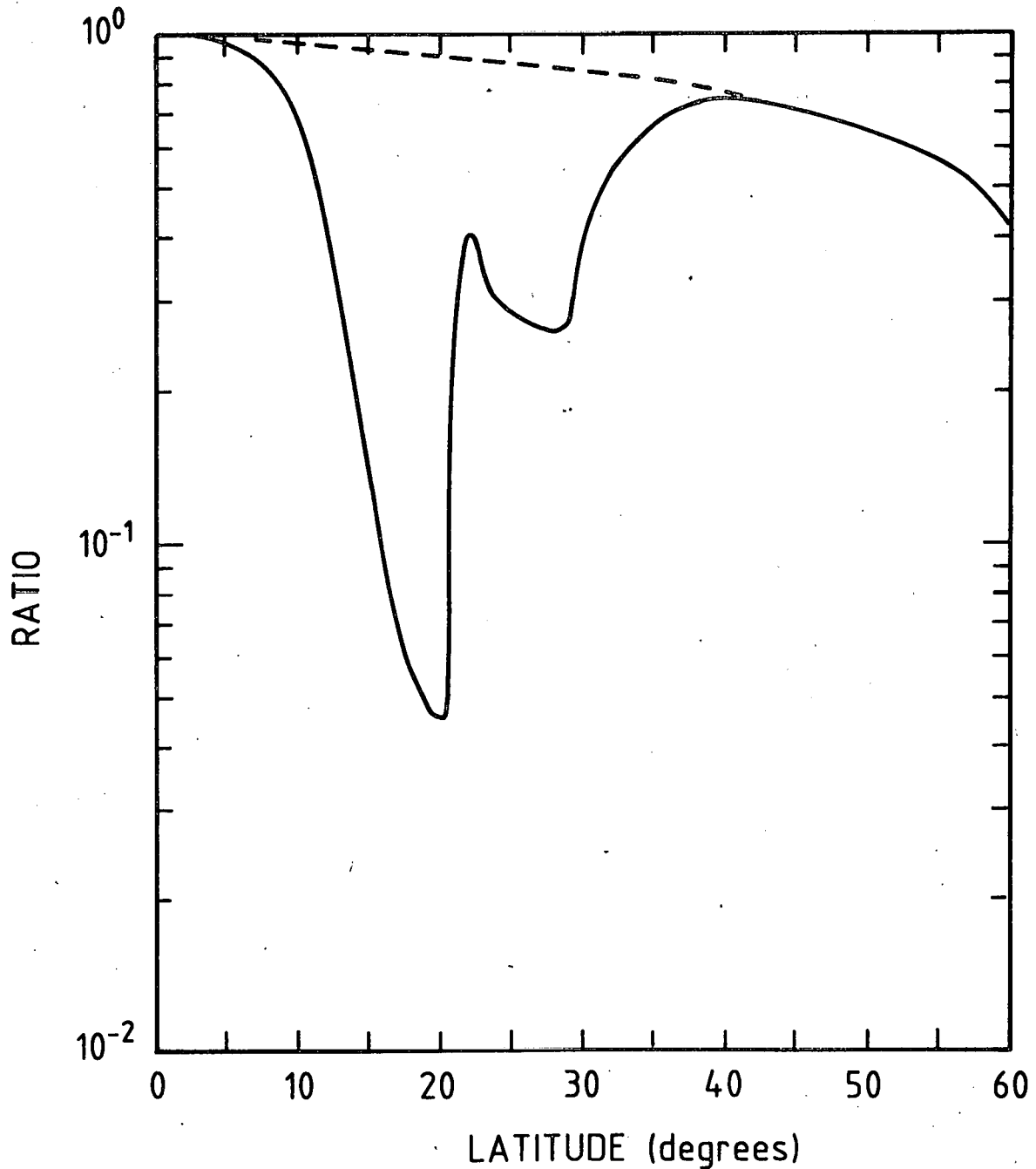


Fig. 5.- Latitudinal variation in the winter hemisphere at a solar longitude of  $45^\circ$  ( $225^\circ$ ) of the ratio of the daily insolation with the oblateness effect and the effect of the ring system ( $I_{D0r}$ ) to the daily insolation without the above mentioned effects ( $I_D$ ) (full line). The ratio ( $I_{D0}/I_D$ ) is also represented (dashed curve).

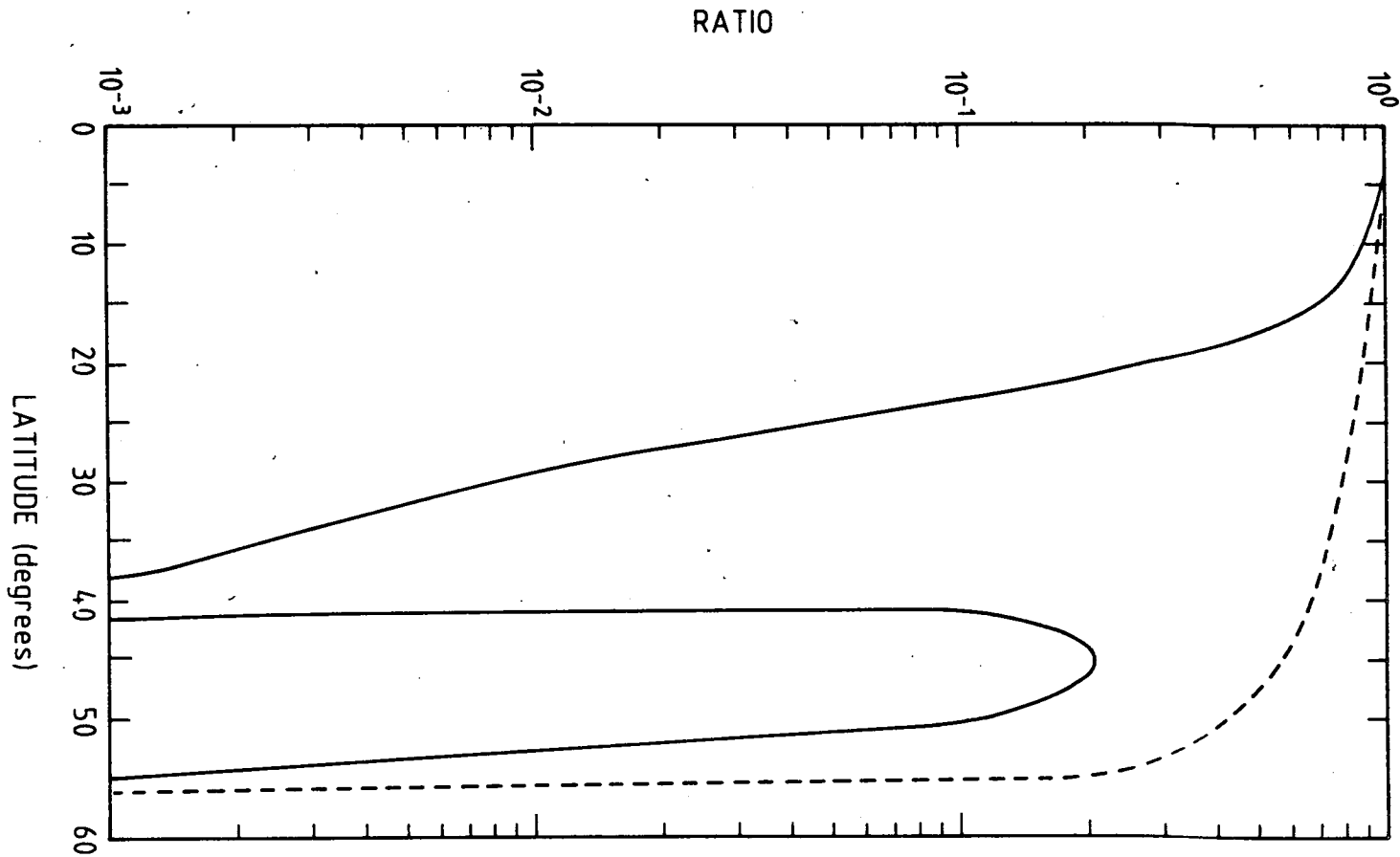


Fig. 6.- Latitudinal variation in the winter hemisphere at winter solstice of the ratio of the daily insolation with the oblateness effect and the effect of the ring system ( $I_{DO_1}$ ) to the daily insolation without the above mentioned effects ( $I_D$ ) (full line). The ratio ( $I_{DO}/I_D$ ) is also represented (dashed curve).

The latitudinal ratio distribution at a solar longitude between autumnal equinox and winter solstice is shown in Figure 5. The ratio of both insolutions ( $I_D$  and  $I_{DO\tau}$ ) amounts to about 20 ( $I_{DO\tau}/I_D = 0.05$ ) at localities equal to  $20^\circ$  latitude. Past of  $40^\circ$ , the influence of the ring system is either unimportant and it is exclusively the oblateness which is responsible for the reduction of the insolation (ratio = 0.76).

The loss of the solar radiation at winter solstice in both hemispheres is even more spectacular as can be deduced from Figure 6. For example, at latitudes of  $23^\circ$ ,  $29^\circ$  and  $38^\circ$ , the corresponding ratios ( $I_{DO\tau}/I_D$ ) are equal to  $10^{-1}$ ,  $10^{-2}$  and  $10^{-3}$ , respectively.

In winter, as for all planets, the effect of the flattening results in a more extensive polar region; the large oblateness of Saturn gives rise to a maximum difference of the two Arctic Circles ( $I_D = 0$ ) and ( $I_{DO} = 0$ ), occurring at winter solstice of approximately  $5^\circ$  as can be seen from Figures 1 and 2 (or 3).

Comparing our results with those of Brinkmann and Mc Gregor (1979) it has to be noted that the general pattern of the insolation curves is in reasonable agreement, although near the solstices and for low- and midlatitudes there are some striking differences particularly for the isocontours 1 and 2  $\text{cal cm}^{-2} (\text{Saturnian day})^{-1}$ . The higher optical depths used in our paper evidently yields attenuations of the solar radiation which are higher than those obtained by the above cited authors, who, for the optical thicknesses of the A, B and C ring used 0.5, 1.0 and 0.1 respectively.

### 3.2. MEAN DAILY INSOLATION

The mean (summer, winter or annual) daily insolutions  $\bar{I}_D$ ,  $\bar{I}_{DO}$  and  $\bar{I}_{DO\tau}$  as a function of latitude are plotted in Figures 7 and 9 (northern hemisphere) and in Figure 11 (both hemispheres), whereas the percentage differences  $100 (\bar{I}_{DO\tau} - \bar{I}_D)/\bar{I}_D$  and  $100 (\bar{I}_{DO} - \bar{I}_D)/\bar{I}_D$  are illustrated in Figures 8, 10 and 12. In figures 10 and 12 the mathematical difference between the two curves is also shown. As in section 2, the bars over symbols signify seasonal (denoted by S and W for summer and winter) or annual (A) averages.

The summer hemispheres being not affected by the ring system, it is obvious that  $(\bar{I}_{DO\tau})_S = (\bar{I}_{DO})_S$ . The increase of insolation between a spherical and an oblate planet Saturn for latitudes less than the subsolar point ( $26.73^\circ$ ) is clearly demonstrated in Figures 7 and 8 (see also Van Hemelrijck, 1982a), the maximum difference occurring at a latitude of about  $12^\circ$  and reaching a value of the order of 1%. Beyond the subsolar point,  $(\bar{I}_{DO\tau})_S = (\bar{I}_{DO})_S < (\bar{I}_D)_S$  and the maximum loss of insolation is found at mid-latitudes ( $50-55^\circ$ ) and is near 3%.

The mean winter daily insolutions are depicted in Figure 9, the corresponding percentage differences in Figure 10. Comparing the mean winter insolutions between a spherical and an oblate planet it can be seen from Figure 10 that the percentage difference increases with increasing latitude up to about  $60^\circ$  and may attain values of about 34%. At higher latitudes the differences remain practically constant. The importance of the shadow effect on the mean winter daily insolation is particularly evident from the Figure. For latitudes between 0 and about

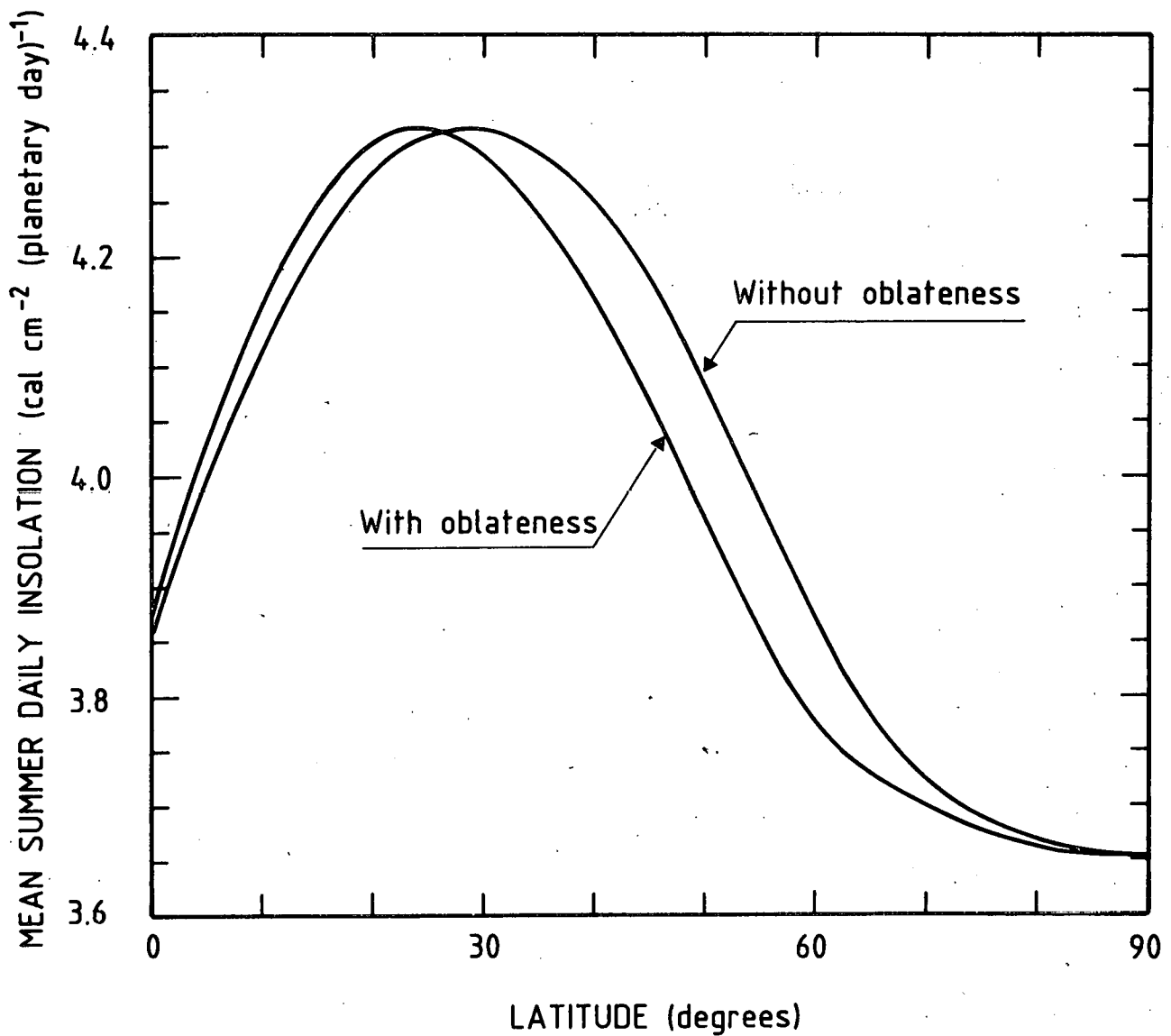


Fig. 7.- Latitudinal variation of the mean summer daily insolations  $(\bar{I}_{D0})_S$  (with oblateness) and  $(\bar{I}_D)_S$  (without oblateness) at the top of the atmosphere of Saturn.

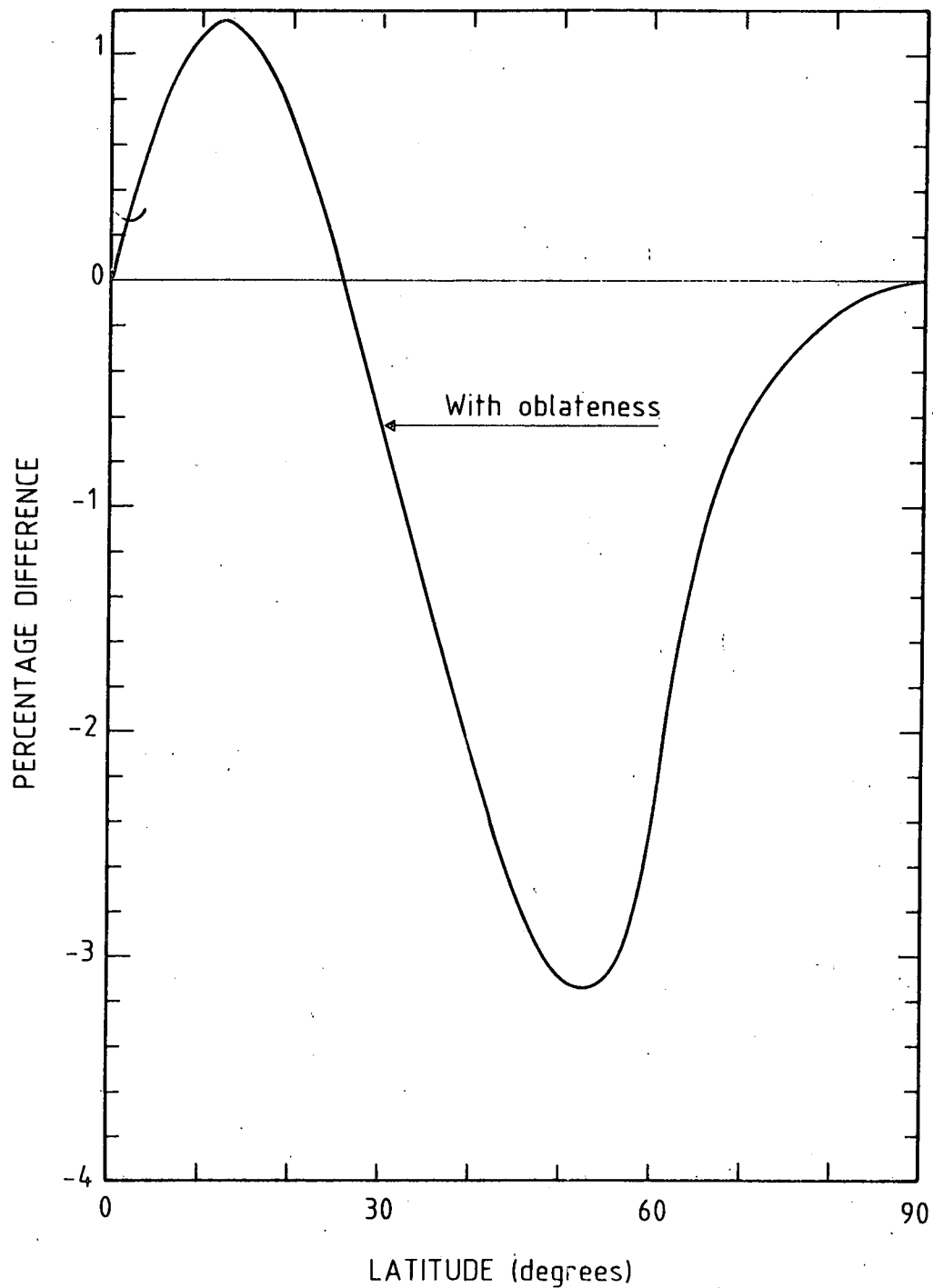


Fig. 8.- Latitudinal variation of the percentage difference  $100 [(\bar{I}_{D0})_S - (\bar{I}_D)_S] / (\bar{I}_D)_S$ . The bars over symbols signify seasonal averages.

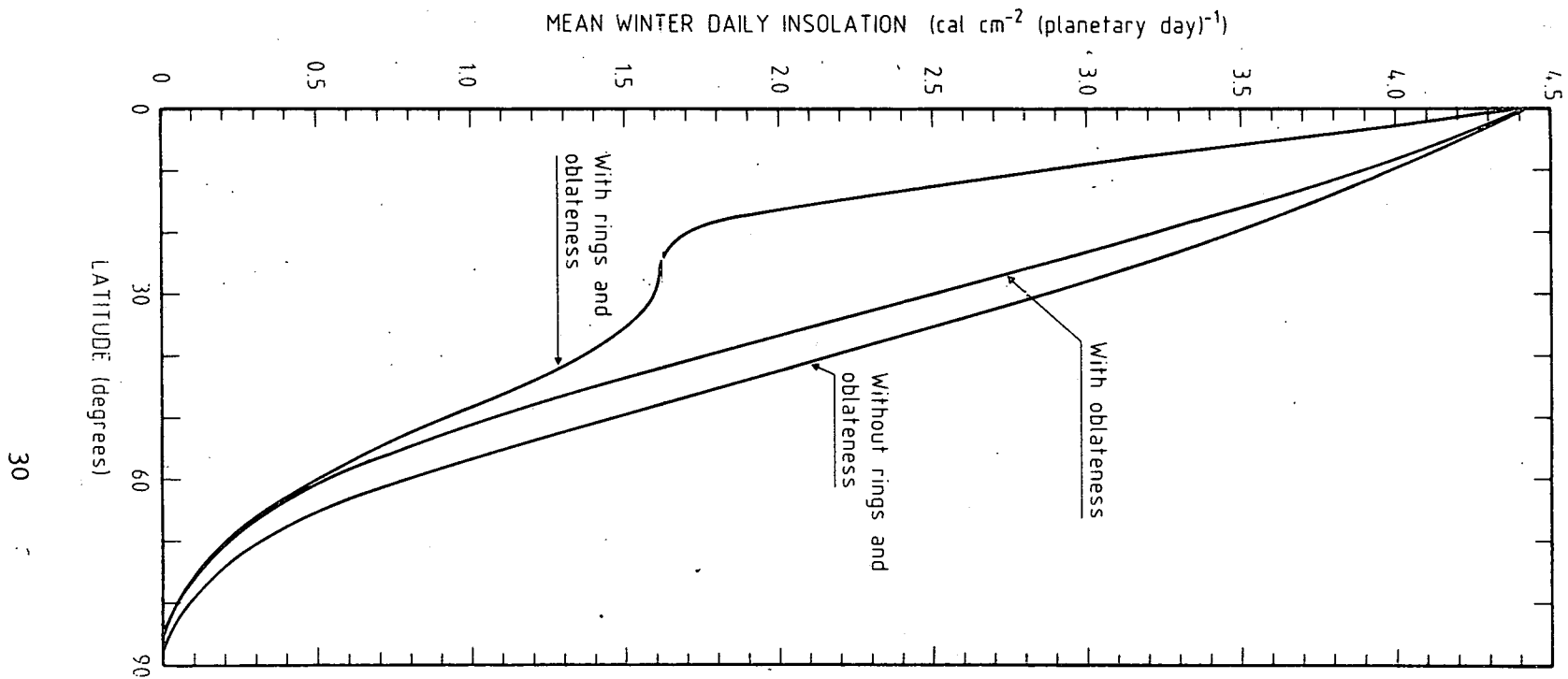


Fig. 9.- Latitudinal variation of the mean winter daily insolations  $(\bar{I}_{DO\tau})_W$  (with rings and oblateness),  $(\bar{I}_{DO})_W$  (with oblateness) and  $(\bar{I}_D)_W$  (without rings and oblateness) at the top of the atmosphere of Saturn.



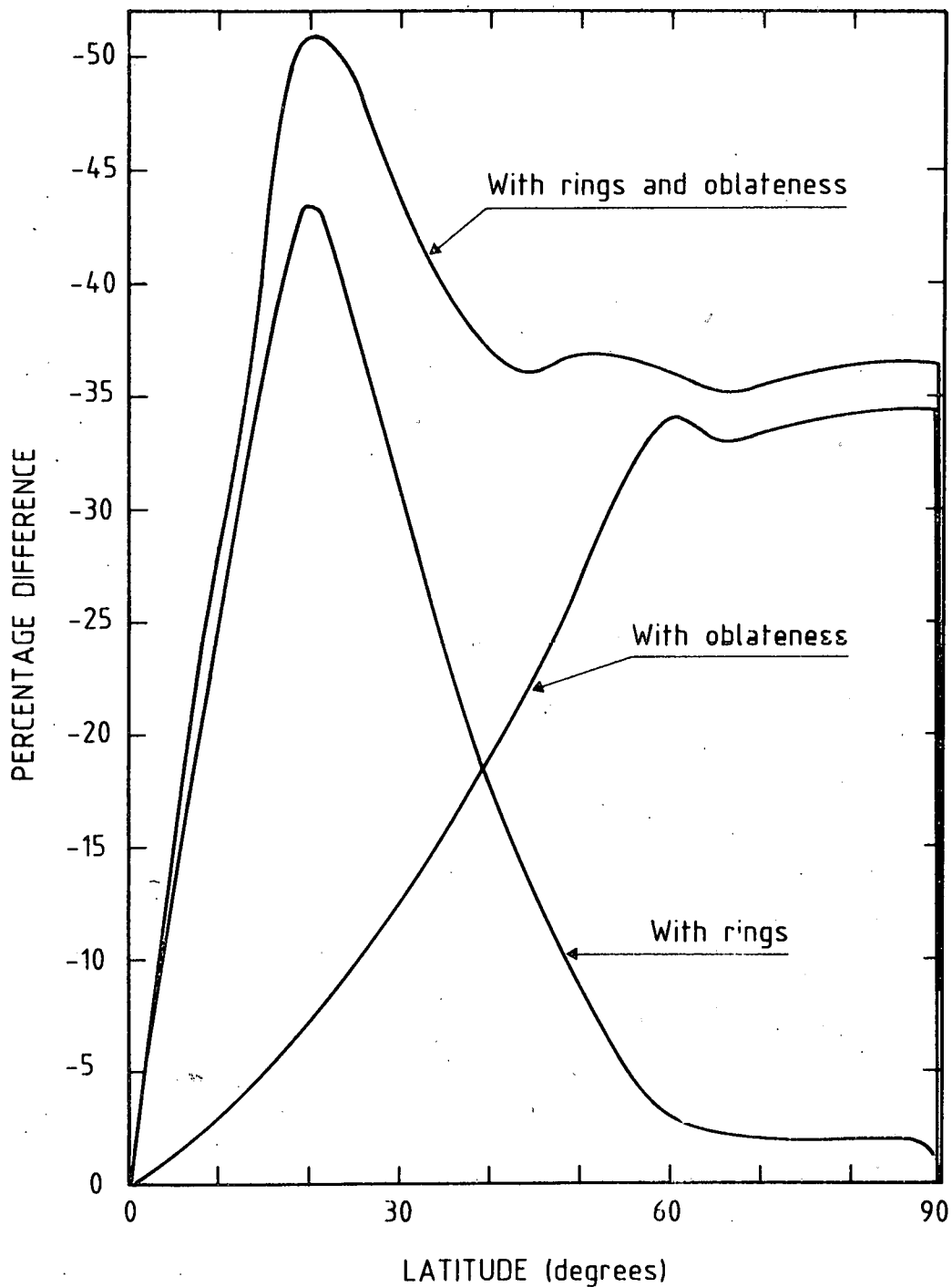


Fig. 10.-Latitudinal variation of the percentage differences  $100[(\bar{I}_{DO\tau})_W - (\bar{I}_D)_W]/(\bar{I}_D)_W$  (with rings and oblateness) and  $100[(\bar{I}_{DO})_W - (\bar{I}_D)_W]/(\bar{I}_D)_W$  (with oblateness). The effect of the rings only is illustrated by the third curve denoted by "with rings".

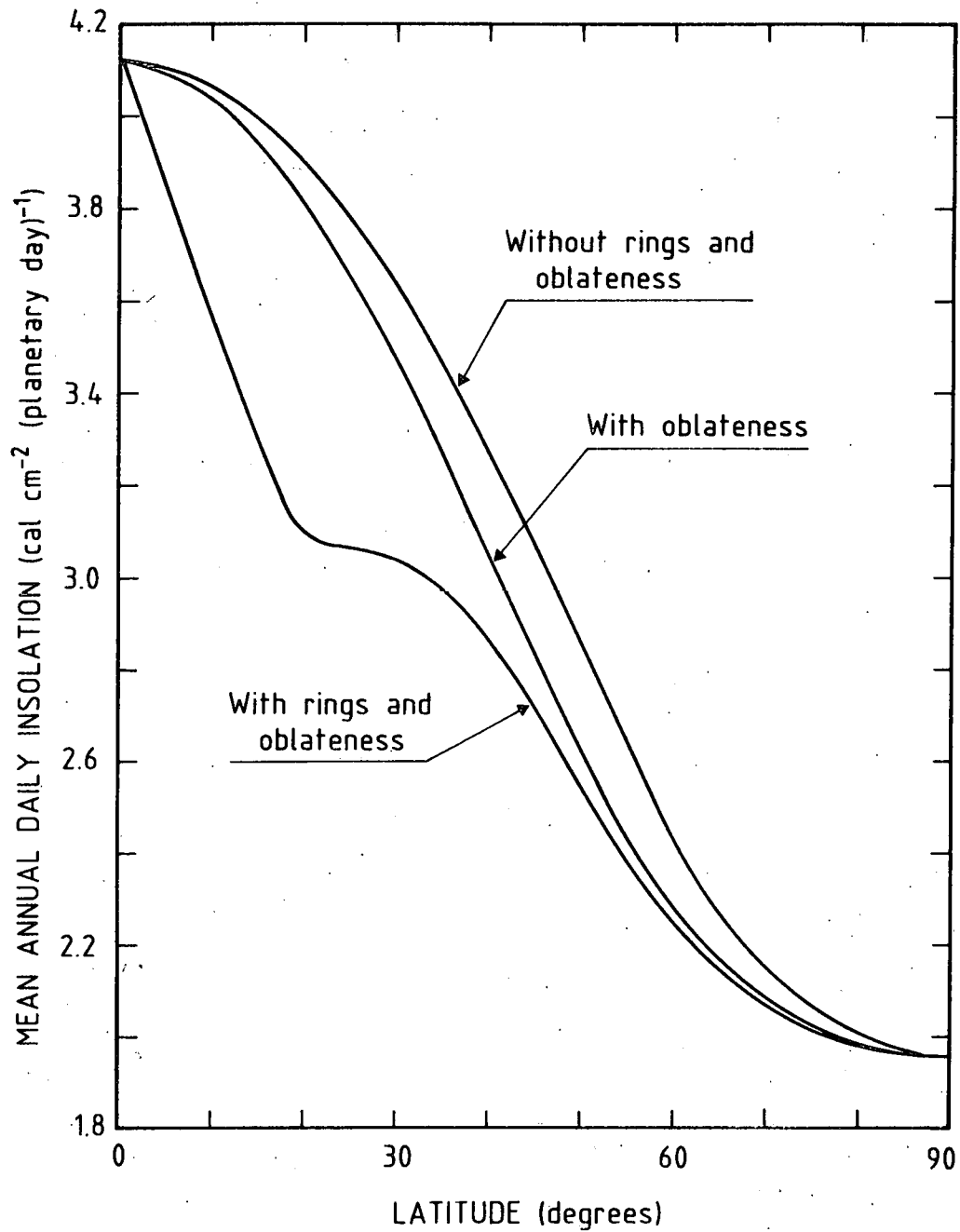


Fig. 11.-Latitudinal variation of the mean annual daily insolations  $(\bar{I}_{DO\tau})_A$  (with rings and oblateness),  $(\bar{I}_{DO})_A$  (with oblateness) and  $(\bar{I}_D)_A$  (without rings and oblateness) at the top of the atmosphere of Saturn.

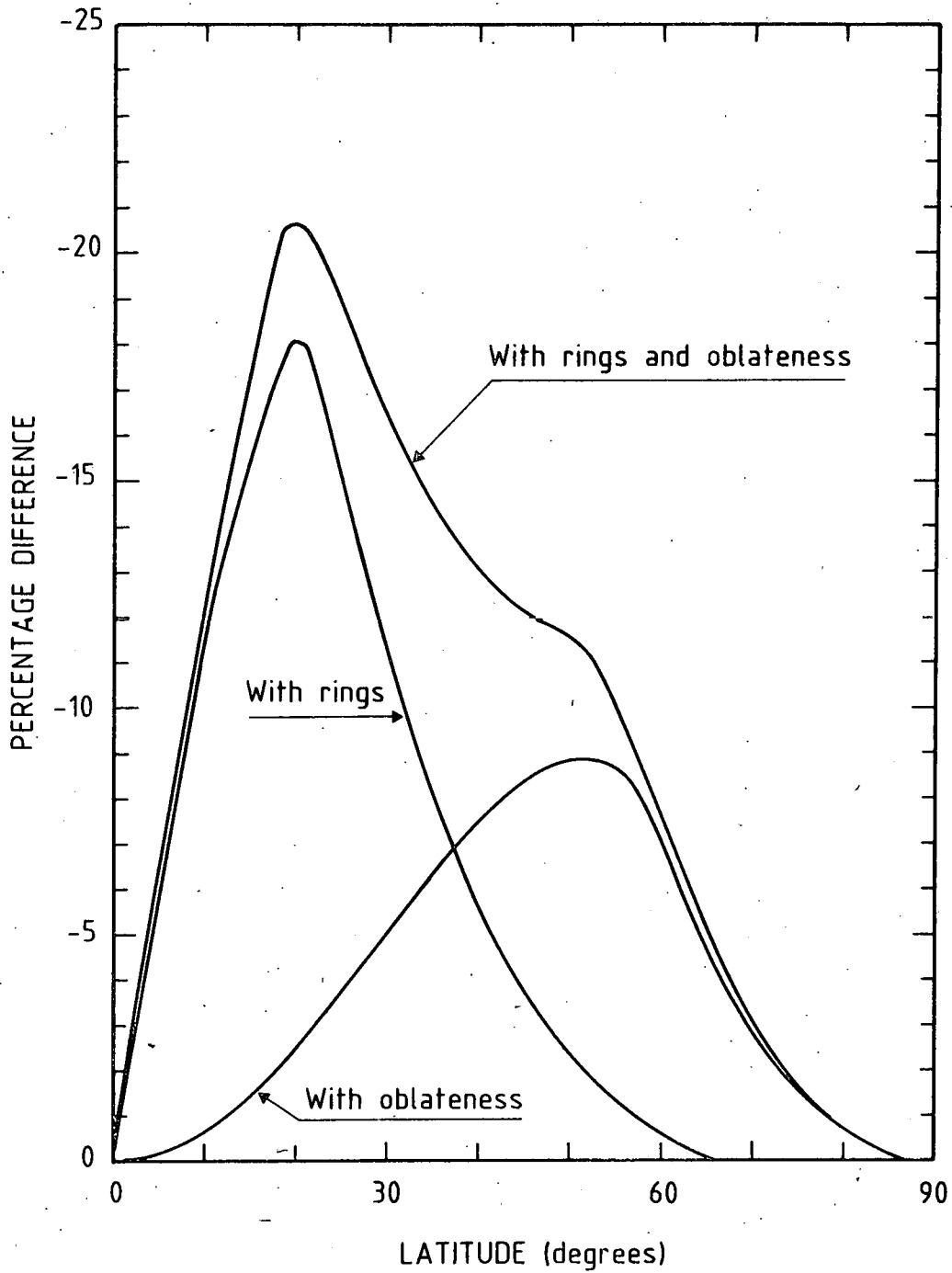


Fig. 12.-Latitudinal variation of the percentage differences  $100[(\bar{I}_{DO\tau})_A - (\bar{I}_D)_A]/(\bar{I}_D)_A$  (with rings and oblateness) and  $100[(\bar{I}_{DO})_A - (\bar{I}_D)_A]/(\bar{I}_D)_A$  (with oblateness). The effect of the rings only is illustrated by the third curve denoted by "with rings".

20° the loss of insolation enhances to approximately 50%, then decreases to about 36% at 45° and finally keeps a nearly constant value up to polar region latitudes where it drops extremely rapid to zero. It is worth noting that poleward of 60°, the two curves representing the mean winter-time insolation closely parallel, the difference being of the order of 2%. For the sake of completeness, the effect of the rings only is also illustrated by the curve denoted by "with rings". The peak percentage difference attains a value of about 43% at  $\lambda_{\odot} = 20^{\circ}$  and the latitude past which the loss of solar energy due to the oblateness effect is greater than the reduction by the ring effect is near 40°.

It is to be emphasized that the Figures 7 and 9 relate to the northern hemisphere. In order to obtain the corresponding values for the southern one, the ordinates of Figure 7 have to be multiplied by the ratio  $T_S$  (northern hemisphere)/ $T_S$  (southern hemisphere) which equals approximately 1.15, whereas the data of Figure 9 have to be multiplied by the factor  $T_W$  (northern hemisphere)/ $T_W$  (southern hemisphere) which amounts about 0.87. Since the percentage differences are symmetric with respect to the planet's equator, a value at a given latitude in Figures 8 and 10 applies to both hemispheres.

The variability of the mean annual daily insulations as a function of latitude is shown in Figure 11; the corresponding percentage differences are plotted in Figure 12. Note that the data from both Figures are valid for the northern as well as for the southern hemisphere. The difference between the mean annual daily insulations  $(\bar{I}_D)_A$  and  $(\bar{I}_{DO})_A$  increases with increasing latitude and reaches a peak value of nearly 9% at a latitude of about 50°. Past of this latitude, the

percentage difference reduces. The importance of the combined effect (rings + oblateness) on the mean annual daily insolation is particularly evident from Figure 12 where it can be seen that the percentage difference is strongly dependent upon the latitude. From 0 to 20°, the loss of insolation enhances nearly linear up to a maximum value of approximately 20% (18% when taking only into account the rings). In their 1979 paper Brinkman and Mc Gregor have noted that "for latitudes between 0 and 30° as much as 14% of the total annual insolation is lost through the shadow effect". At 30, 40 and 50° we found, for the combined effect, percentage differences of 16.6, 13.1 and 11.4% (the corresponding values for which only the rings are responsible amount to about 11.5, 5.7 and 2.5%). Based on the graph figuring in the paper of the above mentioned authors we get the impression that their values are considerably lower. Figure 12 also clearly indicates that the influence of the shadow is almost negligible beyond 55° (equal or less than about 1%). Finally, near 37° the influence of the oblateness is numerically equal to the effect of the ring shadow (~ 7%).

#### 4. CONCLUDING REMARKS

This study clearly demonstrates that the shadow of the ring system of Saturn causes significant variations in both the planetary-wide distribution and the intensity of the daily insolation. The combined effect of the ring shadows and the oblateness decreases the daily solar radiation over much of the winter hemispheres mainly near the solstices (up to mid-latitudes). In the vicinity of the equinoxes the loss of solar energy is principally limited to equatorial and low latitude regions. Furthermore, it is obvious that the summer hemispheres are not affected by the rings.

Concerning the mean winter and annual daily insolutions it is found that the reduction reaches peak values of respectively 50 and 20% at a latitude of  $20^{\circ}$ .

#### ACKNOWLEDGEMENTS

We would like to thank L. Vastenaekel, J. Schmitz and F. Vandreck for their help with the manuscript and the illustrations. The computer assistance of A. Pittonvils and E. Falise is also very much appreciated.

## REFERENCES

- ALLEN, C.W. : 1963, *Astrophysical Quantities*, 2nd ed. Athlone Press, University of London.
- BRINKMAN, A.W. and Mc GREGOR, J. : 1979, *Icarus* 38, 479.
- COOK, A.F., FRANKLIN, F.A. and PALLUCONI, F.D. : 1973, *Icarus* 18, 317.
- DAVIES, M.E., ABALAKIN, V.A., LIESKE, J.H., SEIDELMANN, P.K., SINCLAIR, A.T., SINZI, A.M., SMITH, B.A. and TJUFLIN, Y.S. : 1983, *Cel. Mech.* 29,309.
- ESPOSITO, L.W., O'CALLAGHAN, M. and WEST, R.A. : 1983, *Icarus*, 56, 439.
- LEVINE, J.S., KRAEMER, D.R. and KUHN, W.R. : 1977, *Icarus* 31, 136.
- SMITH, B.A., SODERBLOM, L., BEEBE, R., BOYCE, J., BRIGGS, G., BUNKER, A., COLLINS, S.A., HANSEN, C.T., JOHNSON, T.V., MITCHELL, J.L., TERRILE, R.J., CARR, H., COOK, A.F., II, CUZZI, J., POLLACK, J.B., DANIELSON, G.E., INGERSOLL, A., DAVIES, M.E., HUNT, G.E., MASURSKY, H., SHOEMAKER, E., MORRISON, D., OWEN, T., SAGAN, C., VEVERKA, J., STROM, R. and SUUMI, V.E. : 1981, *Science* 212, 163.
- VAN HEMELRIJCK, E. : 1982a, *Icarus* 51, 39.
- VAN HEMELRIJCK, E. : 1982b, 'The Oblateness Effect on the Solar Radiation Incident at the Top of the Atmosphere of Mars', in *Proceedings of the Workshop on the Planet Mars, Leeds, 1982, ESA Special Publication SP-185*, 59.
- VAN HEMELRIJCK, E. : 1982c, *Bull. Acad. R. Belg., Cl. Sci.* 68, 675.
- VAN HEMELRIJCK, E. : 1983a, *Solar Energy* 31, 223.
- VAN HEMELRIJCK, E. : 1983b, *The Moon and the Planets* 28, 125.
- VAN HEMELRIJCK, E. : 1985a, *Earth, Moon, and Planets*, 33, 157.
- VAN HEMELRIJCK, E. : 1985b, *Earth, Moon, and Planets*, 33, 163.
- VOROB'YEV, V.I. and MONIN, A.S. : 1975, *Atm. Ocean. Phys.* 11, 557.
- WARD, W.R. : 1974, *J. Geophys. Res.* 79, 3375.
- WILLSON, R.C. : 1982, *J. Geophys. Res.* 87, 4319.